Apoptosis (2012) 17:516–527
DOI 10.1007/s10495-011-0690-1

ORIGINAL PAPER

Hepatitis B vaccine induces apoptotic death in Hepa1–6 cells

Heyam Hamza · Jianhua Cao · Xinyun Li · Changchun Li · Mengjin Zhu · Shuhong Zhao

Published online: 17 January 2012

Abstract Vaccines can have adverse side-effects, and these are predominantly associated with the inclusion of chemical additives such as aluminum hydroxide adjuvant. The objective of this study was to establish an in vitro model system amenable to mechanistic investigations of cytotoxicity induced by hepatitis B vaccine, and to investigate the mechanisms of vaccine-induced cell death. The mouse liver hepatoma cell line Hepa1–6 was treated with two doses of adjuvanted (aluminium hydroxide) hepatitis B vaccine (0.5 and 1 μg protein per ml) and cell integrity was measured after 24, 48 and 72 h. Hepatitis B vaccine exposure increased cell apoptosis as detected by flow cytometry and TUNEL assay. Vaccine exposure was accompanied by significant increases in the levels of activated caspase 3, a key effector caspase in the apoptosis cascade. Early transcriptional events were detected by qRT-PCR. We report that hepatitis B vaccine exposure resulted in significant upregulation of the key genes encoding caspase 7, caspase 9, Inhibitor caspase-activated DNase (ICAD), Rho-associated coiled-coil containing protein kinase 1 (ROCK-1), and Apoptotic protease activating factor 1 (Apaf-1). Upregulation of cleaved caspase 3,7 were detected by western blot in addition to Apaf-1 and caspase 9 expressions argues that cell death takes place via the intrinsic apoptotic pathway in which release of cytochrome *c* from the mitochondria triggers the assembly of a caspase activation complex. We conclude that exposure of Hepa1–6 cells to a low dose of adjuvanted hepatitis B vaccine leads to loss of mitochondrial integrity, apoptosis induction, and cell death, apoptosis effect was observed also in C2C12 mouse myoblast cell line after treated with low dose of vaccine (0.3, 0.1, 0.05 μg/ml). In addition In vivo apoptotic effect of hepatitis B vaccine was observed in mouse liver.

Keywords Hepatitis B vaccine · Hepa1–6 cells · Apoptosis · Caspase-dependent pathway · TUNEL · Flow cytometry

Introduction

Recombinant hepatitis B vaccine, in common with many other pharmaceutical products, can have adverse side-effects. Hepatitis B vaccine is prepared from transformed Chinese hamster ovary (CHO) cells expressing hepatitis B virus surface antigen, and the purified antigen in liquid form is rendered insoluble by that addition of aluminum salts. The aluminum compound acts as an adjuvant to dramatically boost the immune reaction to the vaccine and prolong its effects.

A new syndrome termed macrophagic myofasciitis (MMF), comprising diffuse arthromyalgias and fatigue, has been attributed to the aluminum adjuvant in vaccines, and the syndrome has been particularly associated with hepatitis B vaccine and tetanus vaccine. MMF lesions appear to be secondary to intramuscular injection of vaccines containing aluminum hydroxide, and it has been shown that long-term persistence of aluminum hydroxide and an ongoing local immune reaction is present in MMF patients whose systemic symptoms appeared subsequently to

H. Hamza · J. Cao · X. Li · C. Li (✉) · M. Zhu · S. Zhao
Key Lab of Agricultural Animal Genetics, Breeding, and Reproduction of Ministry of Education, College of Animal Science and Technology, Huazhong Agricultural University, Wuhan 430070, People's Republic of China
e-mail: lichangchun@mail.hzau.edu.cn

H. Hamza
e-mail: Heyam68_hamza@yahoo.com

vaccination [1]. Histopathological observations of changes at the injection site in mice were observed over 20 weeks after a single intramuscular (i.m.) injection of aluminum hydroxide-adsorbed tetanus toxoid (Alum-TT) but not after injection of tetanus toxoid (TT) alone. Aluminum adjuvant alone produced marked injury to muscle fibers, and neutrophils infiltration was observed around aluminum remnants; microabscesses have also been reported following i.m. injection of Alum-TT [2].

In addition to local tissue damage, there is evidence that aluminum accumulates in the central nervous system (CNS) and can predispose to neurodegeneration. There is increasing evidence for a link between aluminum neurotoxicity and Alzheimer's disease (AD). Aluminum, as does mercury, activates microglia leading to chronic brain inflammation, a major event in both AD and Parkinson's disease [3]. Flarend and coworkers used radiolabeled aluminum (either aluminum hydroxide or aluminum phosphate) to study the fate of vaccine aluminum injected at a dose approved by the US Food and Drug Administration (0.85 mg per dose). Both these approved vaccine adjuvants led to elevated blood levels of aluminum over 28 days, and raised aluminum levels were also found in the kidney, spleen, liver, heart, lymph nodes and brain [4].

It was previously reported that aluminum can cause cells to undergo programmed cell death or apoptosis, a highly regulated process that is present in all multicellular organisms. Apoptotic cell death has been associated with several chronic conditions including inflammation, malignancy, autoimmunity and neurodegeneration. Apoptotic cell death can be induced by several different toxic agents. Carcinogenic transition metals including cadmium, chromium and nickel are known to promote apoptosis and also DNA base modifications, strand breaks and rearrangements [5].

Apoptosis is generally characterized by distinct morphological characteristics and is considered to be a vital component of diverse processes including normal cell turnover, proper development and functioning of the immune system, hormone-dependent atrophy, and embryonic development. Excess or insufficient apoptosis is a factor in many human conditions including neurodegenerative disease, tissue damage following ischemia, hepatotoxicity, renal toxicity, autoimmune disorders, and many types of cancer [6].

The molecular mechanisms underlying the toxicity of such metals, including aluminum, are not understood. Examination of total mRNA levels in primary human neural cells exposed in vitro to 100 Nanomolar aluminum sulfate using high-density DNA microarrays revealed that seven genes were significantly upregulated, and these were found to encode pro-inflammatory or pro-apoptotic signaling elements, including nuclear factor kappa B (NF-κB) subunits, interleukin (IL)-1β, cytosolic phospholipase A_2, cyclooxygenase-2, beta-amyloid precursor protein (APP) and death-domain associated protein (DAXX), a regulatory protein known to induce apoptosis and repress transcription [7]. Neuro-2a cells treated with aluminium for 24 h showed alterations in apoptosis-related gene expression, and treatment induced cell death via a combination of apoptosis and necrosis [8].

Studies have also revealed that aluminum hydroxide is toxic in vivo. Male outbred CD-1 mice received a subcutaneous injection of a dose equivalent to two human vaccine adjuvant doses. Subsequent immunohistochemistry of spinal cord and motor cortex revealed significantly increased motor neuron apoptosis and raised levels of reactive astrocytes and microglial proliferation in both tissues [9]. Apoptotic neurons were identified in aluminum-injected animals, showed significantly increased activated caspase 3 levels in lumbar spinal cord (255%) and primary motor cortex (192%) compared with the controls [10].

In addition to direct actions on neural cells, aluminum might also cause tissue damage indirectly by stimulating an abnormal generalized immune response. Indeed, adjuvants are selected because of their capacity to boost non-specific immune responsiveness. The neurotoxicity of adjuvants could therefore be due in part to an abnormal immune response; it has been proposed that adjuvants, in conjunction with stress and other factors, can modify the specific type of immune response [11]. In support, aluminum hydroxide was previously shown to stimulate Th2 T-helper cell cytokine responses selectively [12].

The demonstrated neurotoxicity of aluminum hydroxide and its relative ubiquity as an adjuvant suggest that greater scrutiny by the scientific community is warranted [9]. Previous in vivo study was appeared that recombinant hepatitis B vaccine has toxic effect on mouse liver, changed the expression level of inflammation and metabolism genes [13]. In the present study we sought to evaluate the effects of whole hepatitis B vaccine and assess whether Antigen/adjuvant combination exerts collective adverse effect on mouse Hepa1–6 cells and to investigate whether hepatitis B vaccine causes programmed cell death. A central objective has been to establish an in vitro model system that will be useful in defining the pathways and mechanisms involved in vaccine toxicity. We report here that hepatitis B vaccine causes apoptotic cell death via both via caspase-dependent and intrinsic pathways.

Materials and methods

Vaccine

Recombinant and adjuvanted hepatitis B vaccine produced in CHO cells and containing aluminum hydroxide was

manufactured by Huabei Medicine (China) and was purchased from the Institute of Non-Communicable Disease (Wuhan, China).

Animals

Male Kunming mice, weighting 17–20 g, were used in the experiment. Mice were divided into four groups: the first, second and third groups were injected intraperitoneally with 20 μg/ml (one human dose) of hepatitis B vaccine and scarified after 24, 48 and 72 h respectively, fourth group was considered as control mice.

Cell culture and treatment

Mouse hepatoma cell lines Hepa1–6 and mouse myoblast cell line C2C12 were obtained from American Type Culture Collection (ATCC). Cells were maintained at 37°C, 5% CO_2 in a HERA cell 150 humidified incubator (Thermo Scientific, USA). Cells were grown in Dulbecco's modified Eagle medium (DMEM) (Thermo Scientific, USA) supplemented with 10% v/v heat-inactivated fetal bovine serum (Gibco, USA) and 10,000 units/ml streptomycin and penicillin (Genome). Cells (2×10^6 cells/ml) were seeded and exposed to different doses of hepatitis B vaccine (0.125–2 μg protein per ml). Cell viability testing (below) indicated that the median effective dose (ED_{50}) for cell death at 24–72 h was in the range 0.5–1 μg/ml. Separate cultures were therefore treated with either 0.5 or 1 μg/ml of hepatitis B vaccine.

C2C12 were treated with different dose of vaccine (3, 1, 0.05 μg/ml) to study apoptosis by flowcytometry.

Determination of cell viability

A commercial cell viability kit (WST-8; Beyotime, China) was employed to determine cell viability following vaccine treatment. WST-8, a tetrazolium dye, is reduced by NADH produced by mitochondrial transmembrane electron transport to produce soluble formazan; the level of formazan in the culture medium thus provides a measure of mitochondrial integrity. Hepa1–6 cells (2×10^6 per well) were seeded in 96-well plates [14], treated with hepatitis B vaccine, and at different times following treatment (12, 24, 48, and 72 h) 10 μl of WST-8 development solution were added to each well and incubated for a further 2 h at 37°C. The absorbance of each well was read at 450 nm using a commercial ELISA reader (Thermo Labsystems, Finland).

Flow cytometry

Vaccine-treated cell suspensions were fixed with 70% v/v ethanol at 4°C for 24 h, washed with cold PBS, centrifuged ($400 \times g$, 5 min, at 4°C), resuspended in 300–500 μl Propidium iodide (PI)/Triton X-100 staining solution [0.2% v/v Triton X-100 in PBS with 100 μg/ml DNase-free RNase (Biosharp, USA) and 50 μg/ml PI (Biosharp, USA)], and incubated at room temperature for 30 min. PI fluorescence intensity in the stained cells (1×10^4 cells) depend on previous method [14] was determined using a fluorimeter (Beckman Coulter; USA).

TUNEL assay

TUNEL [terminal deoxynucleotidyl transferase (TdT)-mediated dUTP nick-end labeling] was performed using Apo-Direct in situ DNA fragmentation assay kit (Biovision, USA). The detection kit utilizes TdT to catalyze the incorporation of fluorescein-12-dUTP at the free 3′-hydroxyl ends of fragmented DNA. Fluorescein-labeled DNA can then be observed by fluorescence microscopy. Hepatitis B vaccine—treated Hepa1–6 cells were harvested by centrifugation ($300 \times g$), resuspended in 0.5 ml PBS, and fixed by the addition of 5 ml of 1% w/v paraformaldehyde in PBS. After incubation on ice for 15 min on ice, cells were washed with PBS, 5 ml of 70% v/v ethanol was added, and the treated cells were maintained at –20°C for 24 h. Cells were then processed using the Apo-Direct method according to the protocol provided by the manufacturer and analyzed by fluorescence microscopy.

Quantitative RT-PCR

To detect apoptosis-related gene expression, Hepa1–6 cells were treated with 0.5 or 1 μg of vaccine for 48 or 72 h. Total RNA was isolated using TRIzol (Invitrogen), according to the manufacturer's instructions of ferment's kit. First-strand cDNA was synthesized from 2 μg RNA, the final product was diluted fivefold, and aliquots were analyzed by quantitative PCR in 20 μl reactions according to the manufacturer's specifications (Applied Science; Germany). Q-PCR was performed (Roche LightCycler 480; Germany) as follows: initiation at 95°C for 2 min; denaturation at 95°C for 20 s, annealing at different temperatures depending on the primers employed (Table 1), followed by final extension at 72°C for 5 min. Gene expression levels were normalized to those of the internal reference standard (glyceraldehyde 3-phosphate dehydrogenase, GAPDH). Data were analyzed (Excel) to calculate the cycle threshold ΔCT and P values.

Western blot analysis

Caspase 3, Caspase 7, Caspase 9, Apaf-1 and Cytochrome *c* protein expression levels were analyzed by western blotting. Cells were harvested and solubilized in radioimmu-

Table 1 Sequences and annealing temperatures of primers

Gene	Annealing temp. (°C)	Forward primer	Reverse primer
Caspase7	62	5′-GGGAAAGAGGGAGTTAGGTGC-3′	5′-CCAAGGAGTAAAGGTGAGGTGT-3′
Caspase9	56	5′-AACAAAAGTAGGCTCAGGAAC-3′	5′-AATCTGCCACTGCCAACAC-3′
Apaf-1	62	5′-ACCACACCAGAAGAGGGCATCA-3′	5′-CTCGTGTAGCAGAGCGTTGTAGAAT-3′
Rock-1	60	5′-CGGGCAAGAAGGTATCGT-3′	5′-CAACCACCCAAGGCAAC-3′
ICAD	52	5′-GGCACGGATTCACCTGT-3′	5′-GGCTGTCATCACCCAAA-3′

noprecipitation assay (RIPA) lysis buffer with phenylmethylsulfonylfluoride (PMSF). Lysates were clarified by centrifugation (13,000×*g* for 15 min). For cytochrome *c* detection, protein was isolated from mitochondria, cells were collected, washed with ice-cold PBS, and incubated with buffer A (250 mM sucrose, 20 mM Hepes, pH 7.5, 10 mM KCl, 1.5 mM MgCl2, 1 mM EGTA, 1 mM EDTA, 1 mM DTT, 1 mM PMSF, 10 μg/ml each of leupeptin, aprotinin, and pepstatin A) on ice for 30 min. The cells were disrupted by 20 passes through a 26 G needle and centrifuged at 750×*g* for 10 min. The supernatant was centrifuged at 10,000×*g* for 25 min; the pellet containing mitochondria was washed briefly with buffer A and then resuspended with a protein lysis buffer as described above. After centrifugation at 10,000×*g* for 25 min, the supernatant was used as mitochondrial fraction. An equal volume of loading buffer [60 mM Tris–HCl, pH 6.8, 2% sodium dodecyl sulphate (SDS), 10% glycerol, 0.18 M *β*-mercaptoethanol, 0.005% bromophenol blue] was added to each sample, boiled for 5 min and separated by 12.5% polyacrylamide gel electrophoresis in the presence of SDS (SDS–PAGE). Following electrophoresis, proteins were transferred to polyvinyl difluoride (PVDF) membranes (Solarbio, China). Membranes were washed with 0.1% Tween 20 in TBS [140 mM NaCl, 20 mM Tris–HCl pH 7.4] and blocked (5% skim milk, 2 h at room temperature). Blots were developed at 4°C overnight using rabbit anti- cleaved caspase 3 and caspase 7, 9, Apaf-1 and cytochrome *c* antibody according to the manufacturer's instructions (Cell Signaling Technology, USA). Before use, antibodies were diluted 1:1000 in TBS containing 0.1% Tween 20 containing 5% skim milk. After extensive washing, blots were incubated with secondary anti-rabbit antibody for 2 h, washed, and developed using an enhanced chemiluminescence (ECL) system (Thermo Scientific, USA) and exposed to MF-chemiBis camera.

In situ cell death detection

TUNEL staining was performed using in Situ cell death detection kit, POD from (Roche Applied Science, USA). Paraffin sections (3 μm) of mice liver were dewaxed at 60°C for 20 min. Endogenous peroxidase activity was blocked by incubation with 3% hydrogen peroxide for 10–15 min, then slides were incubated with Proteinase K for 15–30 min at 21–37°C. For positive control slides were incubated with DNase grad I for 10 min at 25°C prior to labeling procedures then Tunel reaction solution was prepared [5 μl Tunel—enzyme solution to 45 μl TUNEL—label solution] mixed and added for 1 h at 37°C. Tunel POD was added, incubated at 37°C for 30 min, diaminobenzidine tetrahydrochloride (DAB) chromogen was added, as soon as the sections developed, immersed slides in dH_2O, counterstained sections in hematoxylin, sections were dehydrated, finally slides were examined under light microscope. TUNEL-positive nuclei was carried out in liver sections using a light microscope with an ×40 objective and a pair of ×10 eyepieces. The rate of cell apoptosis was expressed as the percentage of the TUNEL-positive apoptotic nuclei per total nuclei (apoptotic plus non apoptotic) present.

Results

Effect of vaccine on cell viability

Hepa1–6 cells were treated with different doses of hepatitis B vaccine (0.125–2.0 μg/ml) for 12, 24, 48 and 72 h and viability was assessed using a mitochondrial integrity assay. Cytotoxicity was observed at all concentrations tested, and the extent of toxicity was dependent upon both exposure time and vaccine concentration. Figure 1 presents the cell viability following vaccine treatment; a dose of 1 μg/ml was found to decrease cell viability by 50% after 24 h.

Vaccine treatment induces cell death

Hepa1–6 were treated with the indicated doses of hepatitis B vaccine for 24, 48 or 72 h, cell counts treated with propidium iodide, and viable were analyzed by flow cytometry. Induction of cell death was both time- and dose-dependent. As shown in Fig. 2, in the absence of vaccine, only 1.69% of cells underwent cell death (Fig. 2a). By contrast, exposure to 1 μg/ml hepatitis B vaccine caused significant toxicity, with 9.19, 12.11, and 15.94% of cell

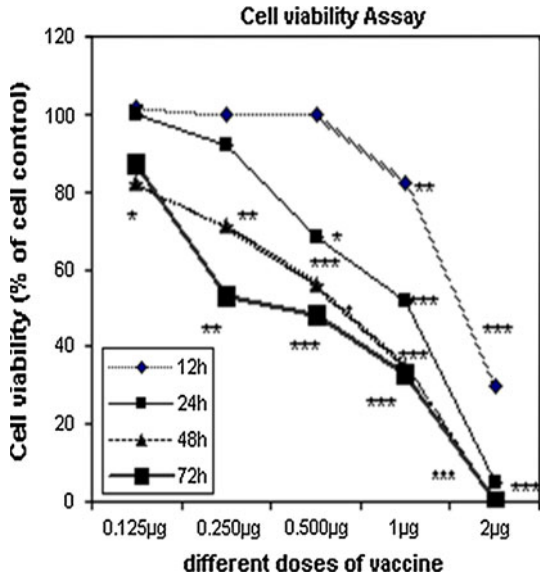

Fig. 1 Hepa1–6 cell viability after 24, 48 or 72 h of hepatitis B vaccine treatment as assessed by the WST-8 assay. Different doses of vaccine (0.125–2.0) µg/ml were employed. Reduced cell viability was both time- and dose-dependent. Values are means ± SD; * $P < 0.05$; ** $P < 0.005$; *** $P < 0.0001$ versus control

death at 24, 48 and 72 h, respectively (Fig. 2e, f, g). Treatment with 0.5 µg/ml hepatitis B vaccine produced a significant increase in cell death only after 48 h (5.84%) and 72 h (7.80%), as shown in Fig. 2c, d, whereas there was no significant increase in cell death following treatment with 0.5 µg/ml for 24 h (Fig. 2b). Percentage of apoptotic cells are presented as mean ± SD. in comparison with the control cells (Fig. 2h). For C2C12, cells were treated with (0.3, 0.1, 0.05 µg/ml) at 24 h, vaccine was induced apoptosis even with low doses (18.02%), (11.31%) and (5.32%) respectively (Fig. 2j, k, l) in comparison with control cells (0.24%) as shown in Fig. 2i. The effect of aluminum hydroxide on cell apoptosis in Hepa1–6 cells was studied separately as shown in Fig. 2. In the absence of aluminum only (0.09%) of cells underwent cell death (Fig. 2o). By contrast, exposure to aluminum hydroxide with 0.125 mg/dose and 0.075 mg/dose appeared significant increase in cell death (0.68%), (0.31%) respectively (Fig. 2m, n).

DNA fragmentation

To address whether cell death resulted from apoptosis, the TUNEL assay was employed to measure DNA fragmentation, a late step following apoptosis induction. No TUNEL-positive apoptotic cells were detected in the absence of vaccine (Fig. 3b). By contrast, TUNEL-positive cells were detected after 24, 48, and 72 h of vaccine exposure at 1 µg/ml (Fig. 3d, f, h). Few apoptotic nuclei were detected after vaccine treatment at 0.5 µg/ml for 24 h (Fig. 3c), whereas significant numbers of apoptotic cells were detected after 48 and 72 h of exposure (Fig. 3e, g).

Vaccine treatment leads to caspase 3, 7, 9, Apaf-1 and cytochrome *c* activation

To investigate the mechanisms of induction of apoptotic cell death we used western blotting to determine the levels of activated caspase after exposure of cells to 1 µg/ml hepatitis B vaccine at 24, 72 h. As shown in Fig. 4, exposure to 1 µg/ml at 72 h had significant effect on caspase 3, 7, 9, Apaf-1 and Cytochrome *c* expression.

Vaccine upregulation of apoptosis-related gene expression

To determine whether vaccine exposure leads to upregulation of the expression of apoptosis-related genes, mRNA expression levels of selected genes were determined after vaccine exposure of Hepa1–6 cells for 48 or 72 h. During apoptosis induction the release of cytochrome *c* from mitochondria triggers the assembly of a caspase activation complex, accompanied by increases in Apaf-1 and caspase 9 expression, leading to apoptosome assembly. This activates the caspase cascade and upregulates caspases 3 and 7, triggering activation of ICAD and ROCK-1 that produce DNA fragmentation and cell-membrane shrinkage. Quantitative real-time PCR (qRT-PCR) was performed for caspase 7, caspase 9, ICAD, ROCK-1 and Apaf-1. As shown in Fig. 5, vaccine treatment was found to produce significant increases in mRNA levels for all apoptosis-related genes tested, and the effect was both dose- and time-dependent.

In situ cell death detection

Visualization of mouse liver sections, apoptosis was detected by Tunel assay (Fig. 6a–e) in comparison to control (Fig. 6b) where no apoptosis was detected, vaccine treatment resulted in activation of apoptosis as early as within 24 h of treatment (Fig. 6c). A further progressive increase after 48 and 72 h (Fig. 6d, e). (f) Quantitative estimation of apoptotic nuclei in mice liver sections.

Discussion

The toxicity of many vaccines has been attributed to the inclusion of chemical additives such as aluminum hydroxide that are intended to boost the immune response to vaccine antigens. Potential toxic mechanisms, notably in the CNS, include induction of inflammation (e.g., microgliosis), interference with cholinergic projections

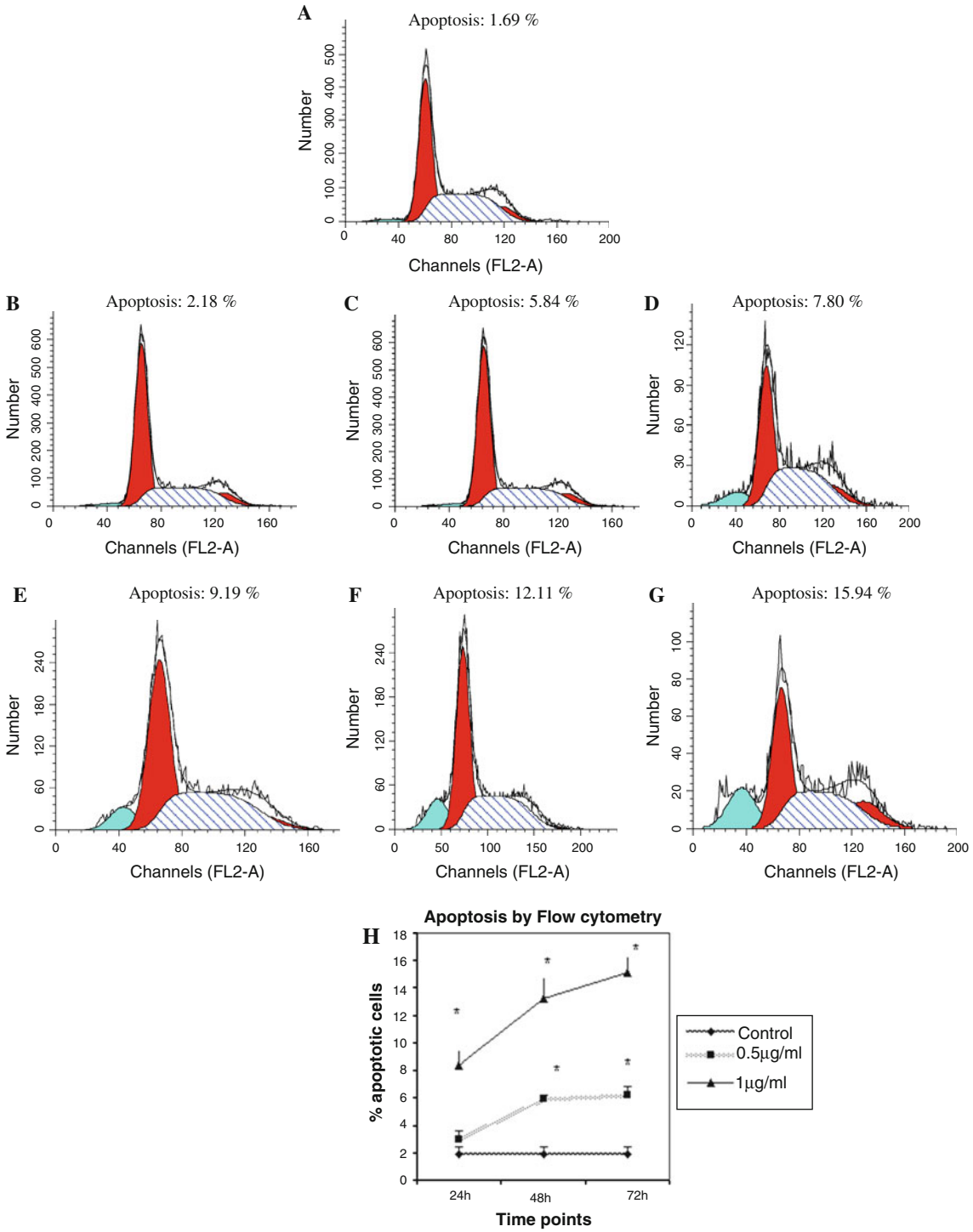

Fig. 2 Detection of apoptotic Hepa1–6 cells after 24, 48 or 72 h and C2C12 cells after 24 h by flow cytometry. **a** Hepa1–6 cells control; **b** 0.5 µg/ml at 24 h; **c** 0.5 µg/ml at48 h; **d** 0.5 µg/ml at 72 h; **e** 1 µg/ml at 24 h; **f** 1 µg/ml at 48 h and **g** 1 µg/ml at 72 h. Hepa cells were stained with PI and analyzed by flow cytometry. In the DNA histogram of FL2A-channel, the first peak represents the apoptosis peak followed by the sub-G_1 peak. **h** Percentages of Hepa1–6 apoptotic cells are presented as means ± SD; * $P < 0.005$ versus control. **j** C2C12 cell treated with 0.3 µg/ml at 24 h, **k** C2C12 treated with 0.1 µg/ml at 24 h, **l** C2C12 treated with 0.05 µg/ml at 24 h, **i** C2C12 control. Hepa1–6 cells were treated with Aluminum hydroxide 0.125 mg/dose, **m** 0.075 mg/dose, **n** control, **o** $P < 0.005$ versus control

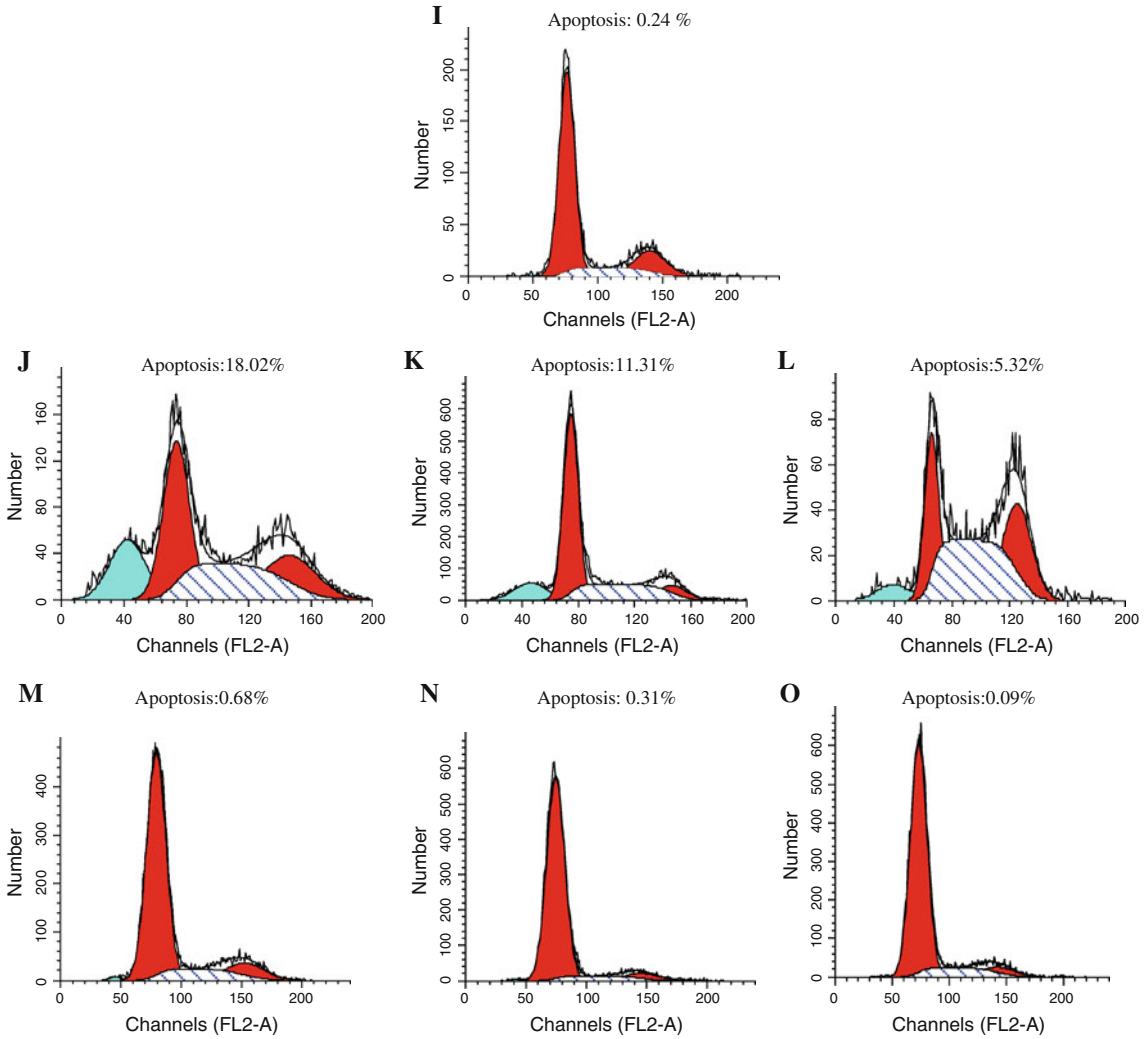

Fig. 2 continued

[15], and reduced glucose utilization [16]. Altered rates of transmembrane diffusion and selective changes in saturable transport systems at the blood–brain barrier (BBB) have also been observed [17]. Aluminum can also induce apoptosis in astrocytes [18] and can provoke glutamate release and excitotoxicity in addition to modifying several enzymatic pathways [19].

The immunostimulatory properties of aluminum salts have recently been shown to be dependent on dendritic cells [20], and the T cell response depends in part on Nalp3 activation [21]. Nalp3 belongs to the nucleotide-binding oligomerization-domain-like (NLR) family of proteins that are involved in the regulation of innate immune responses and cell death pathways. Many NLR family members promote activation of a multiprotein complex termed the inflammasome, leading to the production of proinflammatory caspases [22]. Nalp3, together with ASC (apoptosis-associated speck-like protein containing a caspase recruitment domain) and caspase 1, form the inflammasome which regulates the cleavage and release of the potent pro-inflammatory cytokines IL-1β, IL-18 and IL-33 [23]. Aluminium also induces the production of uric acid, thereby activating the Nalp3 inflammasome and inducing the production of IL-1β and IL-18 [24]. In the liver, aluminum accumulation leads to pathophysiological damage, particularly to the bile duct, and increases alkaline phosphatase levels, a marker of hepatotoxicity [25]. Aluminum has also been reported to induce cholestasis, hepatocellular damage, and impair liver transport function [26].

The present work has sought to establish a reliable in vitro model to evaluate the effects of whole hepatitis B vaccine and assess whether Antigen/adjuvant combination exerts synergistic adverse effect on mouse Hepa1–6 cells and to investigate whether hepatitis B vaccine causes programmed cell death. To facilitate the investigation of the molecular mechanisms underlying vaccine toxicity. Disruption of mitochondrial integrity is thought to play a central role in apoptosis induction [27]. Previous studies on

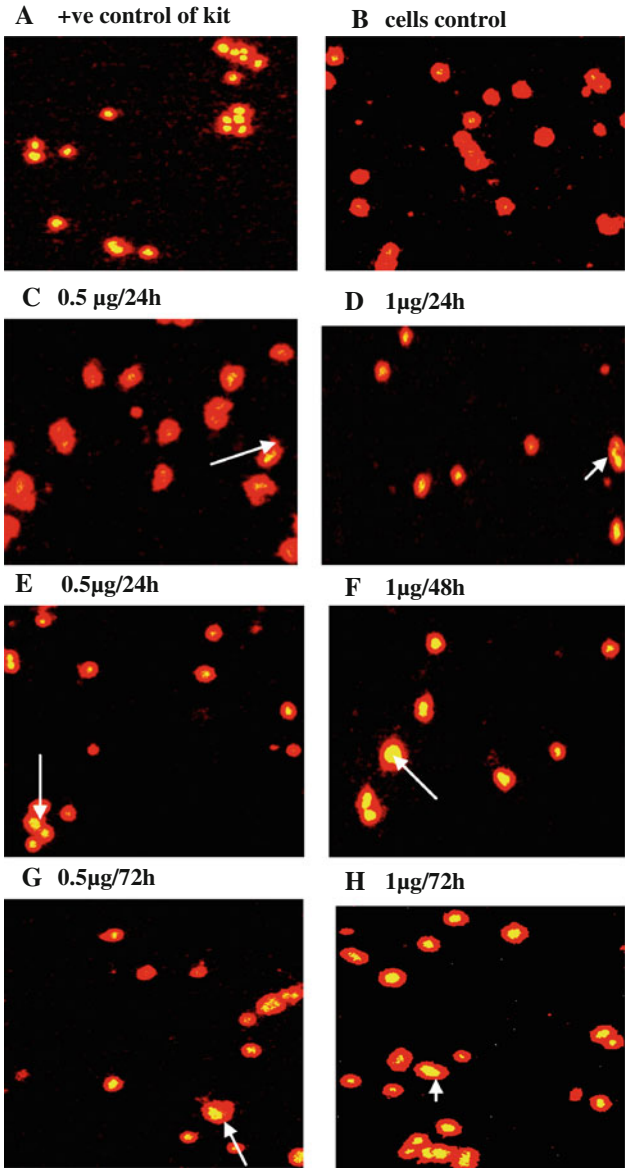

Fig. 3 DNA fragmentation (TUNEL) assay of Hepa1–6 cells treated with 0.5 µg/ml (**c**, **e**, **g**) and 1 µg/ml (**d**, **f**, **h**) of vaccine for 24, 48 and 72 h respectively. **a** Cells with apoptotic nuclei represented positive control of kit, **b** Hepa1–6 cells without treatment served as negative control. *Arrows* indicate nuclei of cells with fragmented DNA

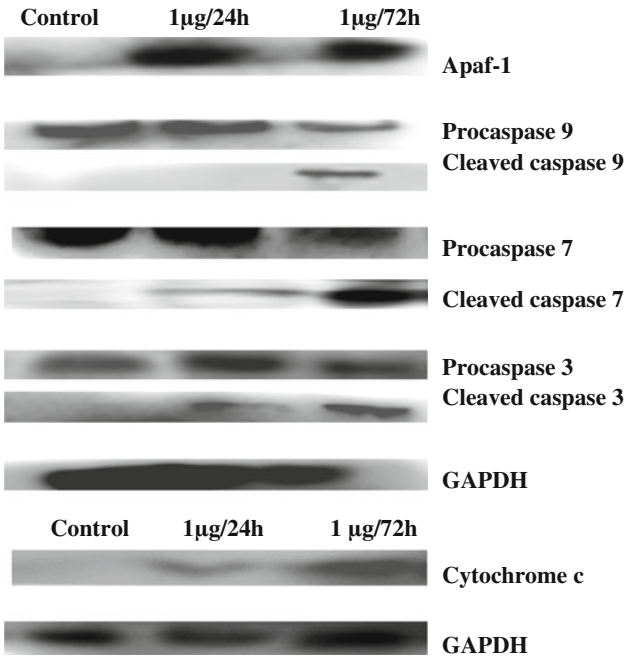

Fig. 4 Representative western blot analysis of caspase 3, caspase 7, caspase 9, Apaf-1 and cytochrome *c* in Hepa1–6 cells, lysates from control cells and cells treated with 1 µg of vaccine for 24or 72 h. Two protein bands of procaspase 9 and cleaved (49 and 39 kDa) were detected using the caspase 9 antibody; Two protein bands of procaspase 7 and cleaved (35 and 20 kDa) were detected using caspase 7 antibody; 17 kDa band represents the activated caspase 3 was detected using cleaved caspase 3 antibody, Apaf-1 (140 kDa) in addition to cytochrome *c*. GAPDH is the loading control

neuroblastoma, glioblastoma, and retinal pigment epithelial cells treated with 1–1,000 µM aluminum chloride reported mitochondrial cytotoxicity and apoptosis, notably at the low aluminum concentrations employed in the present study. Significant apoptotic enzyme activity (caspase 3) was reported in glioblastoma cells 24 h after exposure to 1 µM aluminum [28].

In the present study we used Hepa1–6, and found that adjuvanted hepatitis B vaccine induced mitochondrial cytotoxicity dependent on exposure time and the dose of vaccine. A dose of 1 µg vaccine protein per ml decreased cell viability by 50% after 24 h, as shown by the WST-8 cell viability test, a measure of mitochondrial function. Flow cytometry confirmed cell death induced by treatment with 1 µg/ml vaccine at 24, 48 and 72 h, and similar effect was appeared after treatment of C2C12 with different dose (0.3, 0.1, 0.05 µg/ml) of hepatitis B vaccine. We also report that cell death was associated with significant increases in the levels of activated caspase 3, indicative of apoptosis induction. Caspases are the central executioners of apoptosis that produce the visible changes characteristic of apoptotic cell death, and caspase 3 is thought to be the key caspase enzyme [29]. Our results support previous studies in which raised levels of activated caspase 3 were found in neurons of lumbar spinal cord and primary motor complex of aluminum-injected animals [10].

Cleavage of chromosomal DNA into oligonucleosomal size fragments is a biochemical hallmark of apoptosis. DNA fragmentation has also been reported following aluminum exposure: caspase 3 activation was found to accompanied by nuclear condensation and fragmentation [8], and aluminum-induced degeneration of cortical neurons was associated with DNA fragmentation characteristic of apoptosis [30]. In the present study In vitro TUNEL-positive cells were detected after 24, 48, and 72 h of vaccine exposure at 1 µg/ml hepatitis B vaccine, supported by

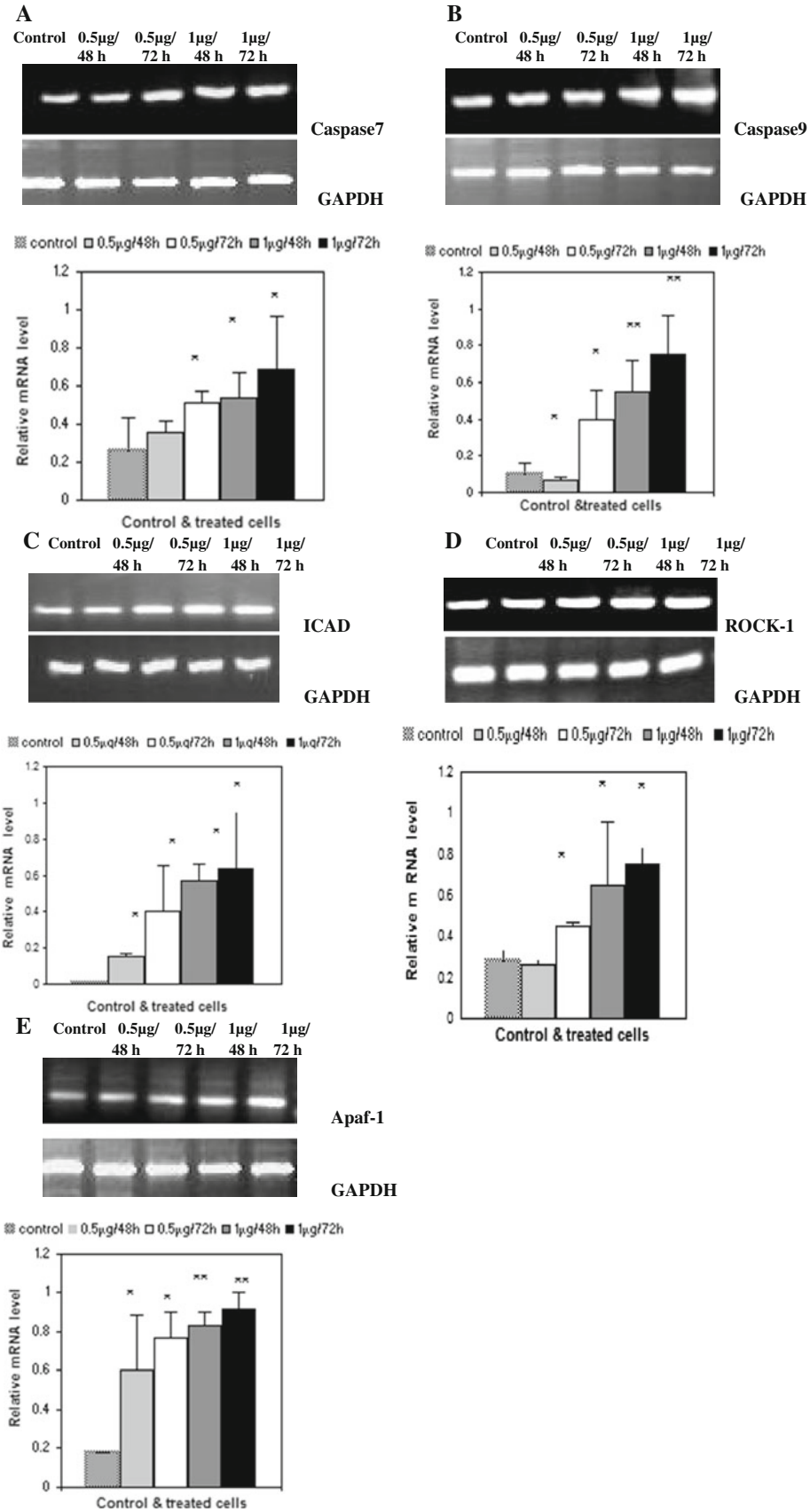

Fig. 5 Early expression of apoptosis-related genes following vaccine treatment. Cells were exposed to vaccine (0.5 or 1 μg/ml) for 48 or 72 h; mRNA expression levels were determined by a quantitative PCR technique employing gene-specific primers. *Top panels*, agarose gels showing RT-PCR products from vaccine-treated cells and controls. *Bottom*; mRNA levels for **a** caspase 7, **b** caspase 9, **c** ICAD, **d** Rock-1, **e** Apaf-1. Results are means ± SD. mRNA levels were normalized to GAPDH; * $P < 0.05$; ** $P < 0.001$ versus control

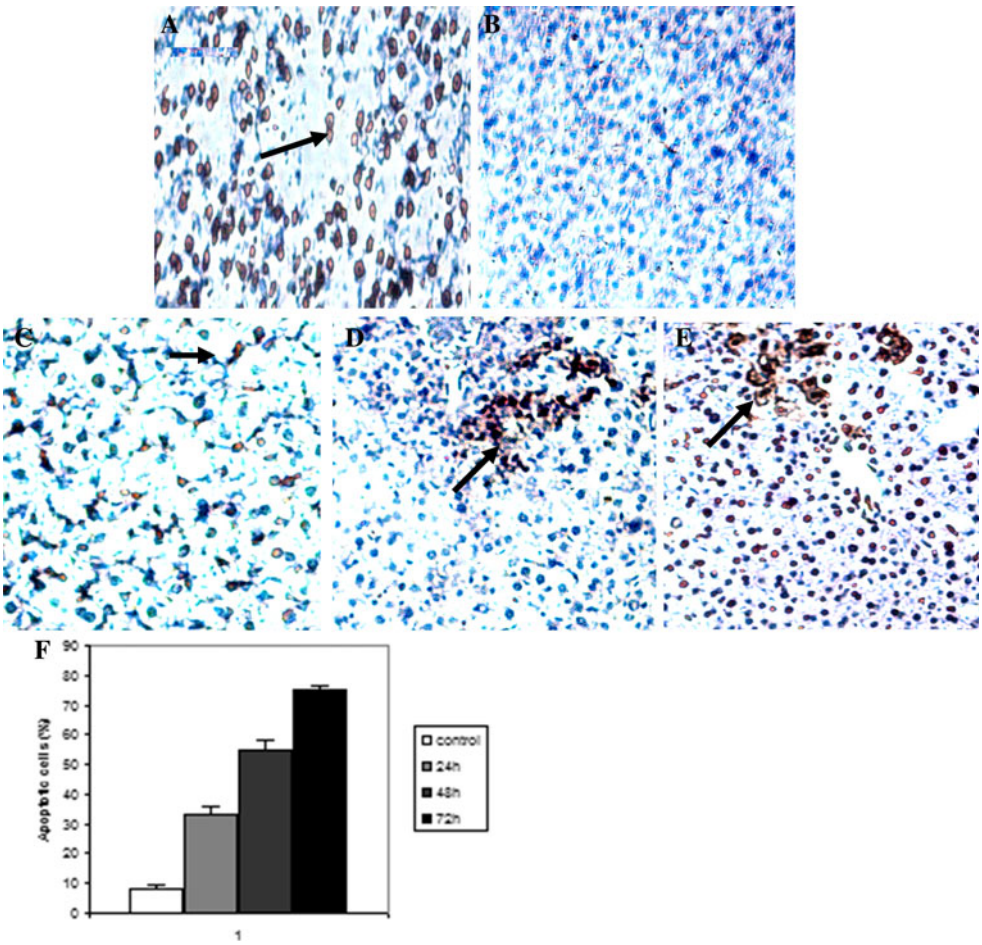

Fig. 6 Detection of DNA fragmentation of mouse liver paraffin sections using the TUNEL method. *Arrows* indicate apoptotic cells. **a** liver section that was pretreated with DNase 1 to nick all DNA, served as positive control. **b** Untreated control, **c** liver section of vaccinated mouse after 24 h, **d** liver section of vaccinated mouse after 48 h, e liver section of vaccinated mouse after 72 h, **f** Quantitative estimation of apoptotic nuclei in mice liver sections.Apoptotic rate was expressed as the percentage of the TUNEL positive nuclei per total nuclei (apoptotic plus non apoptotic). Values are mean ± SEM $P < 0.0001$ versus control

In vivo study in mouse liver suctions after challenging with 20 µg/ml of vaccine, confirming that vaccine exposure causes DNA fragmentation.

We also investigated the underlying molecular mechanisms. A quantitative PCR technique was used to study early transcriptional event of several key apoptosis-related genes as shown in other studies on detection of apoptosis genes such as caspase 9 [31] and apoptotic changes in histopathological evaluation, and genes associated with apoptosis,caspases-2, -3, -9, Apaf-1 and bcl-2, were analyzed by RT-PCR [32]. We report significant increases in mRNA for ICAD/DNA fragmentation factor (DFF45). Upon activation of apoptosis, DFF45 is cleaved by caspase 3, and dissociates from DFF40 [33, 34]. DFF40 (caspase-activated DNase or nuclease, CAD or CPAN) is then activated and cleaves DNA into oligonucleosomal fragments. Subsequent work showed that ICAD (DFF45) could also be activated by caspase 7 [35, 36]. Cell and nuclear shrinkage, chromatin condensation, formation of apoptotic bodies and phagocytosis by neighboring cells characterize the central morphological changes taking place during apoptosis. We also report significant upregulation of Rock-1 gene expression following vaccine exposure. The encoded protein is thought to be responsible for cell shrinkage and is associated with nuclear fragmentation and plasma-membrane blebbing [37].

Gene expression analysis confirms that mitochondria are likely to play a key role in vaccine-induced cell death. The key regulator, Apaf-1, exists as a monomeric protein in the cytoplasm that is incapable of activating caspases [41]. Mitochondrial disruption leads to release of cytochrome *c* into the cytoplasm; this then forms a complex with cytosolic Apaf-1 and activates caspase 9 [38, 39] and caspase 3 [40]. Caspase 9 is directly responsible for the activation of downstream caspases 3 and 7 [42]. Apaf-1 thereby functions as a sensor for cell damage by detecting the release of a common mitochondrial protein that is not found in the cytosol of healthy cells [41]. The involvement of this apoptotic cascade in vaccine-induced cytotoxicity is confirmed by mRNA analysis demonstrating significant upregulation of the genes encoding Apaf-1, caspase 7 and caspase 9, combined with raised levels of activated caspase 3.

In conclusion, this study has demonstrated that there is increase in apoptotic cells percentage with the increase of aluminum concentration but less than the collective effect of hepatitis B antigen and aluminum in whole vaccine

which is a potent inducer of apoptotic cell death in Hepa1–6 cells in vitro. Our results confirm that loss of mitochondrial integrity and caspase induction are centrally involved in vaccine-induced cell death.

Acknowledgments This research was supported by National Natural Science Foundation of China and the creative team project of Education Ministry (IRT-0831) and by the Fundamental Research Funds for the Central Universities from Education Ministry of China (2009PY001). We thank Yang Feng, Niu Lili, Wei Wei and GU Ting, in our lab for suggestions on data analysis.

References

1. Gherardi RK, Coquet M, Cherin P, Belec L, Moretto P, Dreyfus PA et al (2001) Macrophagic myofasciitis lesion assesses long-term persistence of vaccine-derived aluminum hydroxide in muscle. Brain 124:1821–1831
2. Goto N, Akama K (1982) Histopathological studies of reactions in mice injected with aluminum-adsorbed tetanus toxoid. Microbiol Immunol 26(12):1121–1132
3. Good PF, Perl DP, Bierer LM, Schmeidler J (1992) Selective accumulation of aluminum and iron in the neurofibrilary tangles of Alzheimer' disease. Ann Neurol 31(3):286–292
4. Richard EF, Stanley LH, Joe LW, David E, Mark AS, Anita C et al (1997) In vivo absorption of aluminum- containing vaccine adjuvants using 26Al. Vaccine 15:1314–1318
5. Rana SV (2008) Metals and apoptosis: recent developments. J Trace Elem Med Biol 22(4):262–284
6. Elmore S (2007) Apoptosis: a review of programmed cell death. Toxicol Pathol 35(4):495–516
7. Walter JL, Maire EP, Theo PK (2005) Nanomolar aluminum induces pro-inflammatory and pro-apoptotic gene expression in human brain cells in Primary culture. J Inorg Biochem 99(9):1895–1898
8. Johnson VJ, Kim SH, Sharma RP (2005) Aluminum-maltolate induces apoptosis and necrosis in neuro-2a cells: potential role for p53 signaling. Toxicol Sci 83(2):329–339
9. Shaw CA, Petrik MS (2009) Aluminum hydroxide injections lead to motor deficits and motor neuron degeneration. J Inorg Biochem 103(11):1555–1562
10. Petrik MS, Wong MC, Tabata RC, Garry RF, Shaw CA (2007) Aluminum adjuvant linked to Gulf War illness induces motor neuron death in mice. Neuromol Med 9(1):83–100
11. Rook GA, Zumla A (1997) Gulf War syndrome: is it due to a systemic shift in cytokine balance towards a Th2 profile? Lancet 349(9068):1831–1833
12. Valensi Jp, Carlson JR, Van Nest GA (1994) Systemic cytokine profiles in BALB/c mice immunized with trivalent influenza vaccine containing MF59 oil emulsion and other advanced adjuvants. J Immunol 153(9):4029–4039
13. Hamza H, Cao J, Li X, Zhao S (2011) In vivo study of hepatitis B vaccine effects on Inflammation and metabolism gene expression. Mol Biol Rep. doi:10.1007/s11033-011-1090-x. 21 Jun 2011
14. Son YO, Jang YS, Heo JS, Chung WT, Choi KC, Lee JC (2009) Apoptosis-inducing factor plays a critical role in caspase independent, pyknotic cell death in hydrogen peroxide-exposed cells. Apoptosis 14(6):796–808
15. Platt B, Fiddler G, Riedel G, Henderson Z (2001) Aluminum toxicity in the rat brain: histochemical and immunocytochemical evidence. Brain Res Bull 55(2):257–267
16. Joshi JG (1990) Aluminum, a neurotoxin which affects diverse metabolic reactions. Biofactors 2(3):163–169
17. Kaya M, Kalayci R, Arican N, Küçük M, Elmas I (2003) Effect of aluminum on the blood-brain barrier permeability during nitric oxide-blockade-induced chronic hypertension in rats. Biol Trace Elem Res 92(3):221–230
18. Aremu DA, Meshitsuka S (2005) Accumulation of aluminum by primary cultured astrocytes from aluminum amino acid complex and its apoptotic effect. Brain Res 1031(2):284–296
19. Nayak P, Chatterjee AK (2001) Effects of aluminum exposure on brain glutamate and GABA systems: an experimental study in rats. Food Chem Toxicol 39(12):1285–1289
20. Kool M, Pétrilli V, De Smedt T, Rolaz A, Hammad H, van Nimwegen M et al (2008) Cutting edge: alum adjuvant stimulates inflammatory dendritic cells through activation of the NALP3 inflammasome. J Immunol 181(6):3755–3759
21. Eisenbarth SC, Colegio OR, O'Connor W, Sutterwala FS, Flavell RA (2008) Crucial role for the Nalp3 inflammasome in the immunostimulatory properties of aluminium adjuvants. Nature 453(7198):1122–1126
22. Sutterwala FS, Ogura Y, Flavell RA (2007) The inflammasome in pathogen recognition and inflammation. J Leukoc Biol 82(2): 259–264
23. Sutterwala FS, Ogura Y, Szczepanik M, Lara-Tejero M, Lichtenberger GS, Grant EP et al (2006) Critical role for NALP3/CIAS1/Cryopyrin in innate and adaptive immunity through its regulation of caspase-1. Immunity 24(3):317–327
24. Kool M, Soullié T, van Nimwegen M, Willart MA, Muskens F, Jung S et al (2008) Alum adjuvant boosts adaptive immunity by inducing uric acid and activating inflammatory dendritic cells. J Exp Med 205(4):869–882
25. Osinska E, Kanoniuk D, Kusiak A (2004) Aluminum hemotoxicity mechanisms. Ann Univ Mariae Curie Sklodowska Med 59(1):411–416
26. Gonzalez MA, Alvarez Mdel L, Pisani GB, Bernal CA, Roma MG, Carrillo MC (2007) Involvement of oxidative stress in the impairment in biliary secretory function induced by intraperitoneal administration of aluminum to rats. Biol Trace Elem Res 116(3):329–348
27. Fiskum G, Starkov A, Polster BM, Chinopoulos C (2003) Mitochondrial Mechanisms of neural cell death and neuroprotective interventions in Parkinson's disease. Ann N Y Acad Sci 991: 111–119
28. Toimela T, Tahti H (2004) Mitochondrial viability and apoptosis induced aluminum, mercuric mercury and methyl mercury in cell lines of neural origin. Arch Toxicol 78(10):565–574
29. Kaufmann SH, Hengartner MO (2001) Programmed cell death: alive and well in the new millennium. Trends Cell Biol 11(12):526–534
30. Fu HJ, Hu QS, Lin ZN, Ren TL, Song H, Cai CK et al (2003) Aluminum-induced apoptosis in cultured cortical neurons and its effect on SAPK/JNK signal transduction pathway. Brain Res 980(1):11–23
31. Huang X, Hazlett LD (2003) Analysis of *Pseudomonas aeruginosa* corneal infection using an oligonucleotide microarray. Invest Ophthalmol Vis Sci 44(8):3409–3416
32. Kijima K, Toyosawa K, Yasuba M, Matsuoka N, Adachi T, Komiyama M et al (2004) Gene expression analysis of the rat testis after treatment with di (2-ethylhexyl) phthalate using cDNA microarray and real-time RT-PCR. Toxicol Appl Pharmacol 200(2):103–110
33. Nagata S (2000) Apoptotic DNA fragmentation. Exp Cell Res 256(1):12–18
34. Sakahira H, Enari M, Nagata S (1998) Cleavage of CAD inhibitor in CAD activation and DNA degradation during apoptosis. Nature 391:196–199
35. Thomas DA, Du C, Xu M, Wang X, Ley TJ (2000) DFF45/ICAD can be directly process by granzyme B during the induction of apoptosis. Immunity 12:621–632

36. Halenbeck R, MacDonald H, Roulston A, Chen TT, Conroy L, Williams LT (1998) CPAN, a human nuclease regulated by the caspase-sensitive inhibitor DFF45. Curr Biol 8(9):537–540
37. Coleman ML, Sahai EA, Yeo M, Bosch M, Dewar A, Olson MF (2001) Membrane blebbing during apoptosis results from caspase-mediated activation of ROCK I. Nat Cell Biol 3(4):339–345
38. Zou H, Henzel WJ, Liu X, Lutschg A, Wang X (1997) Apaf-1, a human protein homologous to *C. elegans* CED-4, participates in cytochrome *c*-dependent activation of caspase-3. Cell 90(3): 405–413
39. Joza N, Susin SA, Daugas E, Stanford WL, Cho SK, Li CY et al (2001) Essential role of the mitochondrial apoptosis—inducing factor in programmed cell death. Nature 410(6828):549–554
40. Li P, Nijhawan D, Budihardjo I, Srinivasula SM, Ahmad M, Alnemri ES et al (1997) Cytochrome c and dATP-dependent formation of Apaf-1/caspase-9 complex initiates an apoptotic protease cascade. Cell 91(4):479–489
41. Acehan D, Jiang X, Morgan DG, Heuser JE, Wang X, Akey CW (2002) Three-dimensional structure of the apoptosome: implications for assembly, procaspase-9 binding and activation. Mol Cell 9(2):423–432
42. Slee EA, Harte MT, Kluck RM, Wolf BB, Casiano CA, Newmeyer DD et al (1999) Ordering the cytochrome *c*-initiated caspase cascade: hierarchical activation of Caspases-2, -3, -6, 7, -8, and -10 in a caspase-9-dependent manner. J Cell Biol 144(2):281–292